FATIGUE CRACK GROWTH OF TITANIUM ROTOR ALLOYS IN VACUUM AND AIR

R. C. McClung
Southwest Research Institute
P. O. Drawer 28510
San Antonio, TX 78228-0510

B. H. Lawless
GE Aircraft Engines
One Neumann Way
Cincinnati, OH 45215

M. Gorelik, C. Date, and Y. Gill
AlliedSignal Engines
P. O. Box 52181
Phoenix, AZ 85072-2181

R. S. Piascik
NASA Langley Research Center
Hampton, VA 23681-2199

Abstract

An enhanced life management system for aircraft turbine engine rotors based on probabilistic damage tolerance methods is currently under development by the engine industry and the FAA, with an initial focus on fatigue cracking at hard alpha (HA) defects in titanium. Since HA defects are usually subsurface, any resulting cracks are embedded and hence isolated from the atmosphere (i.e., vacuum-like) for at least some of their life. Fatigue crack growth (FCG) tests have been conducted in vacuum at various temperatures and stress ratios for Ti-6Al-4V and Ti-6Al-2Sn-4Zr-2Mo+Si rotor alloys. A brief study of vacuum levels suggests that pressures of 10^{-6} Torr are adequate to capture full vacuum effects on FCG rates. Vacuum FCG results are compared with available air data. The vacuum data demonstrate temperature and stress ratio effects comparable to air data. The vacuum and air data exhibit the same growth rates in the upper Paris regime, but apparent thresholds are significantly higher in vacuum than in air.

The current safe-life philosophy for life management of commercial aircraft gas turbine rotors does not account for undetected material and manufacturing anomalies. The engine industry, through the Rotor Integrity Sub-Committee (RISC) of the Aerospace Industries Association (AIA), is currently developing an enhanced life management process based on probabilistic damage tolerance methods and employing opportunity inspections. Southwest Research Institute and four U. S. aircraft engine manufacturers are teamed on an FAA program to provide enhanced predictive tool capability and supplementary material/anomaly behavior characterization and modeling to support the enhanced life management process.

The current program focus is reduction of the risk from melt-related anomalies called hard alpha (HA), which are small zones in the microstructure where the alpha phase has been stabilized by the presence of nitrogen that can be introduced at various stages in the melting history. These hard zones are brittle, usually have cracks and voids associated with them, and have been responsible for the initiation of low-cycle fatigue cracks that resulted in disk failures. Although HA occurrence rates are extremely low and inspection techniques are improving, HA most commonly occurs at subsurface locations, where undetected fatigue cracks can potentially nucleate and grow. Since these cracks are not exposed to the atmosphere, they grow in a vacuum-like environment.

Numerous researchers have noted a difference between FCG rates in air and vacuum for titanium alloys [1-10]. However, these investigations have generally been limited to a single stress ratio (typically $R = 0.1$) and a single temperature (typically ambient). Information on systematic changes in vacuum behavior with stress ratio or temperature is not available. Of greater significance for the current application, insufficient vacuum data are available to support a complete lifing system for FCG in turbine engine rotors, and therefore it is difficult to accurately evaluate the risk associated with crack nucleation at subsurface HA anomalies.

It is also not clear from the literature what vacuum level is adequate to maintain the "full" effect of vacuum on FCG rates. Irving and Beevers [2] cited general evidence for other materials of the existence of a critical pressure below which no further effect on growth rates would be observed with changes in vacuum pressure. The only evidence they could cite for titanium was unpublished research of James on Ti-5Al-2½Sn, where no difference was found between FCG rates at 10^{-5} Torr and $3(10)^{-8}$ Torr. Sugano et al. [11] found that the total fatigue lives of notched commercially pure titanium were an order of magnitude longer at 10^{-5} Torr compared to slightly higher pressures. Bache et al. [10] found no difference in FCG rates for Ti-6Al-4V between lab air and 10^{-2} Torr pressures, but a large difference at 10^{-6} Torr.

Materials and Test Procedures

Experiments were conducted on two rotor-grade titanium alloys, Ti-6Al-4V and Ti-6Al-2Sn-4Zr-2Mo+Si. Both alloys were triple VAR melted and alpha + beta forged, solution heat treated below the beta transus, rapidly cooled, and then aged. The resulting microstructures are shown in Figure 1. All specimens were machined from actual production forgings. Room temperature tensile properties were σ_{YS} = 140 ksi, σ_{ULT} = 152 ksi, 37% RA, 15% elongation for the Ti-6-4, and σ_{YS} = 133 ksi, σ_{ULT} = 145 ksi, 35% RA, 18% elongation for the Ti-6-2-4-2.

A brief study of vacuum level effects was conducted on the Ti-6Al-4V at NASA Langley Research Center. The study employed an ultra high vacuum chamber with an assortment of pumps and gages capable of a wide range of pressures down to $3(10)^{-10}$ Torr. Constant ΔK FCG tests were conducted at 400°F (204°C) and f = 0.33 Hz with a pin-loaded extended compact tension specimen [12], also known as the extended single edge cracked tension

specimen. Fatigue crack length was monitored continuously via crack mouth opening compliance with visual confirmation via a long focal length optical microscope at 400×.

Vacuum FCG rate tests were conducted for a matrix of multiple temperatures and stress ratios on the Ti-6Al-4V (at General Electric Aircraft Engines, GEAE) and the Ti-6Al-2Sn-4Zr-2Mo+Si (at AlliedSignal Engines, AE). Although the tests were conducted at different sites, similar test procedures were followed. Region II (Paris regime) tests were conducted with small surface crack tension, SC(T), specimens, also known as Kb bar specimens [13]. These specimens had a nominal gage section of 168 × 400 mils (GEAE) or 226 × 450 mils (AE) with a semi-circular EDM notch of approximate dimensions 7 × 14 mil (GEAE) or 10 × 20 mil (AE) in the center of the wide face. Tests in the near-threshold regime were conducted at AE on the same SC(T) geometry and at GEAE on single edge notch button head (SENBH) specimens with a 100 mil × 400 mil gage section and a 15 mil EDM notch.

Crack lengths were monitored using the DC electric potential drop method [13], with crack sizes post-test corrected from visual measurements of marked initial and final crack dimensions on the fracture surfaces. Stress intensity factors were calculated from the Newman-Raju solution [14] for SC(T) and the Harris solution [15] for SENBH. Tests were conducted under either constant load or constant ΔK-gradient (increasing or decreasing) at constant R, where the ΔK-gradient was as high as ±20/inch (AE) or ±30/inch (GEAE). Unpublished research at the engine companies has indicated that these gradients, which are more severe than the recommendations of ASTM E647, do not significantly influence the measured growth rates, and are necessary to obtain adequate data on the small specimens. Crack growth rates were calculated with incremental polynomial methods. Vacuum levels were better than 10^{-7} Torr for all tests. Test frequencies were either 1 Hz (some ambient and 400°F tests) or 0.33 Hz (all other tests). Brief studies found no difference in growth rates between these two frequencies at the conditions where the faster frequency was employed.

Results

Sample results from the brief NASA Langley vacuum level study are shown in Figure 2 for ΔK = 18 ksi√in, R = 0.05. The graph of crack length vs. cycles highlights extremely small changes in *da/dN* under constant ΔK and different vacuum levels. Because it is difficult to maintain a perfectly constant vacuum level, each region of crack growth is characterized by a range of vacuum levels. A factor of two reduction in *da/dN* was observed when the vacuum was changed from 10^{-4} to 10^{-5} Torr, but negligible variations in growth rates were observed for vacuum levels ranging from 10^{-5} to 10^{-9} Torr. A test at ΔK = 9 ksi√in, R = 0.5 found no significant variation in *da/dN* between vacuum levels of 10^{-6} and 10^{-9} Torr, but a clear increase in *da/dN* at 10^{-5} Torr. Obviously, this brief, informal study does not definitively resolve the vacuum level question, and further testing at much lower growth rates (very near threshold) would be of particular value. However, the limited data available suggest that vacuum levels better than 10^{-6} Torr should be adequate to capture full vacuum effects for engineering purposes, and, therefore, the 10^{-7} Torr or better levels employed at GE and AE are sufficient.

Vacuum FCG results for Ti-6-4 at 75°F and 400°F (24°C and 204°C) for stress ratios of R = 0, 0.5, and 0.75 are shown in Figures 3 and 4. The data demonstrate typical stress ratio and temperature effects for this material in air. Changing temperature from 75°F to 400°F does not affect vacuum FCG rates significantly except at the highest mean stresses (R = 0.75).

Vacuum FCG rates for Ti-6-2-4-2 at 75°F, 600°F, and 1000°F (24°C, 316°C, and 538°C) for stress ratios of R = 0.05, 0.5, and 0.75 are shown in Figures 5-7. Again, the data demonstrate

typical stress ratio and temperature effects. Mean stress effects are more pronounced at higher temperatures. No temperature effects are evident between 75°F and 600°F at R = 0.05 and 0.5, but temperature effects are seen at all stress ratios for 1000°F and at R = 0.75 for 600°F.

The significance of the vacuum behavior becomes much clearer when compared directly with FCG rate data in laboratory air. Representative comparisons of the vacuum data with the trends of relevant air data from the Damage Tolerant Design Handbook (DTDH) [16] are shown in Figures 8-12. In each case, the vacuum and air data exhibit the same growth rates in the upper Paris regime. The vacuum FCG rates are considerably slower in the near-threshold regime, and the apparent thresholds under vacuum conditions are significantly higher than under ambient conditions. Similar vacuum vs. air trends were seen at all combinations of material, stress ratio, and temperature where available data permitted direct comparisons, including elevated temperature tests with Ti-6Al-2Sn-4Zr-2Mo+Si. These trends are in agreement with the literature data cited earlier at lower stress ratios and temperatures.

These vacuum data are adequate to develop rotor lifing systems with FCG equations as functions of R and T. The equations can be integrated with distributions of HA size and occurrence rate, probability of detection curves, inspection schedules, and rotor stress histories to estimate the reliability of actual hardware with subsurface defects, transitioning to air properties as cracks break through to the surface. The probabilistic design code DARWIN (Design Analysis of Rotors With INspection) being developed at SwRI in the same FAA program performs this FCG life calculation and risk summation from finite element stress history data.

Acknowledgements

This work is funded by the Federal Aviation Administration. The guidance and encouragement of Mr. Bruce Fenton and Mr. Joseph Wilson of the William J. Hughes Technical Center and Mr. Timoleon Mouzakis of the New England Regional Center are gratefully acknowledged, along with the assistance of SwRI Program Manager Dr. Gerald Leverant. Dr. Yi-Der Lee and Ms. Patty Soriano of SwRI are thanked for their help in preparing the manuscript.

References

1. D. A. Meyn, “An Analysis of Frequency and Amplitude Effects on Corrosion Fatigue Crack Propagation in Ti-8Al-1Mo-1V,” Metallurgical Transactions, 2 (1971), 853-865.

2. P. E. Irving and C. J. Beevers, “The Effect of Air and Vacuum Environments on Fatigue Crack Growth Rates in Ti-6Al-4V,” Metallurgical Transactions, 5 (1974), 391-398.

3. H. Doker and D. Munz, “Influence of Environment on the Fatigue Crack Propagation of Two Titanium Alloys,” The Influence of Environment on Fatigue (London: MEP Ltd, 1977), 123-130.

4. J. A. Ruppen and A. J. McEvily,” “Influence of Microstructure and Environment on the Fatigue Crack Growth Fracture Topography of Ti-6Al-2Sn-4Zr-2Mo-0.1Si,” Fractography and Materials Science, ASTM STP 733, (1981), 32-50.

5. M. Peters, A. Gysler, and G. Lutjering, “Influence of Texture on Fatigue Properties of Ti-6Al-4V,” Metallurgical Transactions, 15A (1984), 1597-1605.

6. S. J. Gao, G. W. Simmons, and R. P. Wei, "Fatigue Crack Growth and Surface Reactions for Titanium Alloys Exposed to Water Vapor," Materials Science and Engineering, 62 (1984), 65-78.

7. L. S. Vesier and S. D. Antolovich, "Fatigue Crack Propagation in Ti-6242 as a Function of Temperature and Waveform," Engineering Fracture Mechanics, 37 (1990), 753-775.

8. R. Foerch, A. Madsen, and H. Ghonem, "Environmental Interactions in High-Temperature Fatigue Crack Growth of Ti-1100," Metallurgical Transactions, 24A (1993), 1321-1332.

9. J. Petit, W. Berata, and B. Bouchet, "Fatigue Crack Growth Behavior of Ti-6Al-4V at Elevated Temperature," Titanium '92 Science and Technology, (Warrendale, PA: TMS, 1993), 1819-1826.

10. M. R. Bache, W. J. Evans, and M. McElhone, "The Effects of Environment and Internal Oxygen on Fatigue Crack Propagation in Ti-6Al-4V," Materials Science and Engineering, A234-236 (1997), 918-922.

11. M. Sugano, S. Kanno, and T. Satake, "Fatigue Behavior of Titanium in Vacuum," Acta Metallurgica, 37 (1989), 1811-1820.

12. R. S. Piascik, J. C. Newman, Jr., and J. H. Underwood, "The Extended Compact Tension Specimen," Fatigue and Fracture of Engineering Materials and Structures, 20 (1997), 559-563.

13. R. H. Van Stone and T. L. Richardson, "Potential-Drop Monitoring of Cracks in Surface-Flawed Specimens," Automated Test Methods for Fracture and Fatigue Crack Growth, ASTM STP 877, (1983), 148-166.

14. J. C. Newman, Jr., and I. S. Raju, "Stress Intensity Factor Equations for Cracks in Three-Dimensional Finite Bodies," Fracture Mechanics: Fourteenth Symposium—Volume 1, ASTM STP 791, (1983), I-238-I-265.

15. D. O. Harris, "Stress Intensity Factors for Hollow Circumferentially Notched Round Bars," Journal of Basic Engineering, 89 (1967), 49-54.

16. Damage Tolerant Design Handbook, WL-TR-94-4053, CINDAS/USAF (1994), Vol. 2.

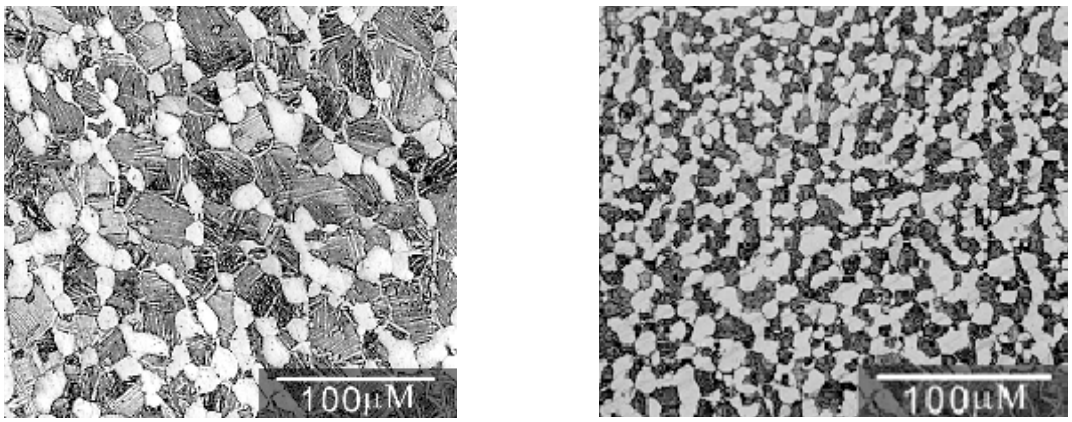

Figure 1. Microstructures of Ti-6Al-4V (left) and Ti-6Al-2Sn-4Zr-2Mo+Si (right)

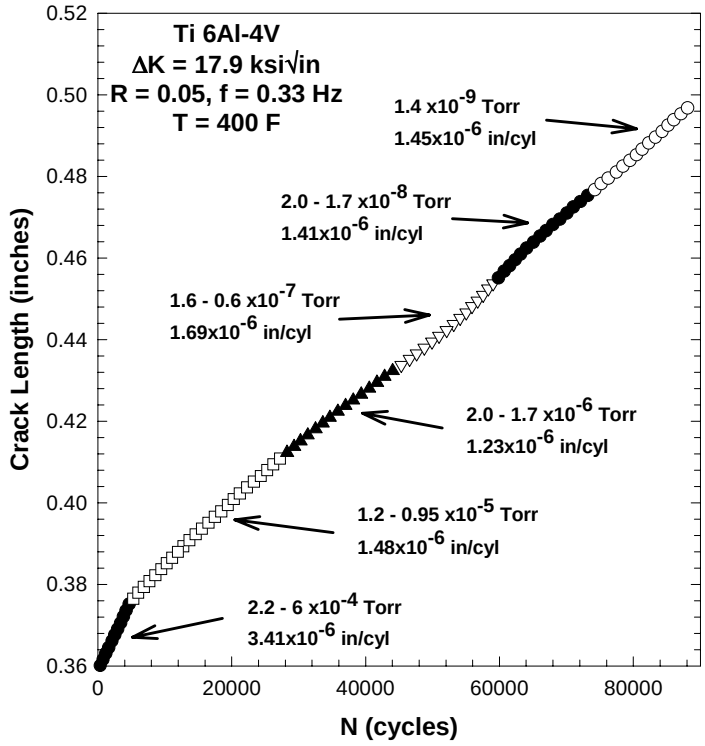

Figure 2. Fatigue crack growth data for Ti-6Al-4V at constant Δ*K* and different vacuum levels

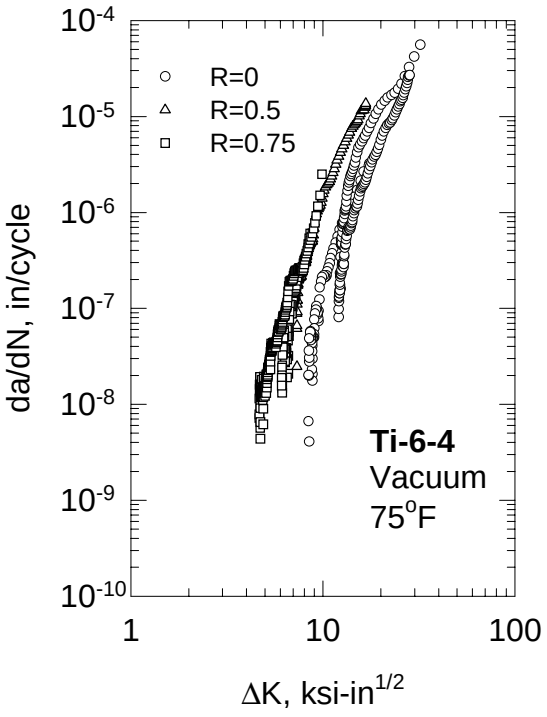

Figure 3. Vacuum FCG data for Ti-6Al-4V at 75°F (24°C)

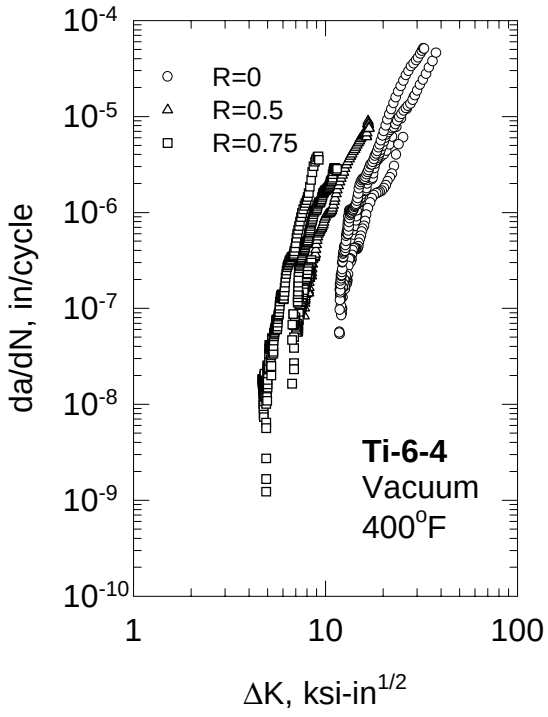

Figure 4. Vacuum FCG data for Ti-6Al-4V at 400°F (204°C)

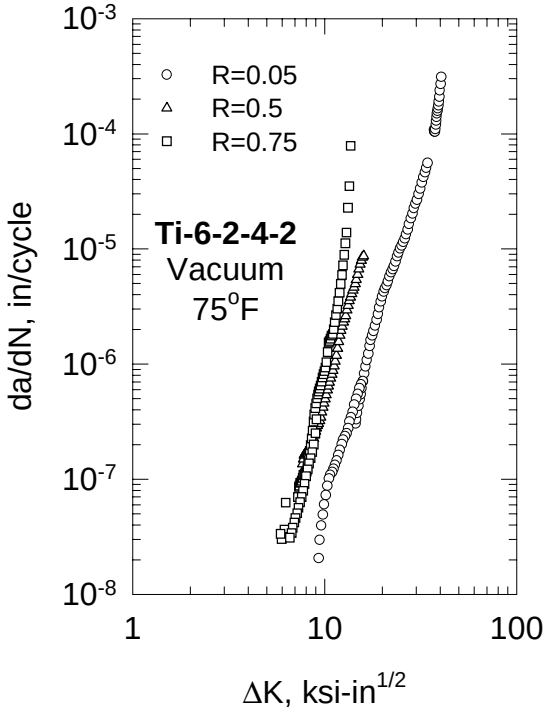

Figure 5. Vacuum FCG data for Ti-6Al-2Sn-4Zr-2Mo+Si at 75°F (24°C)

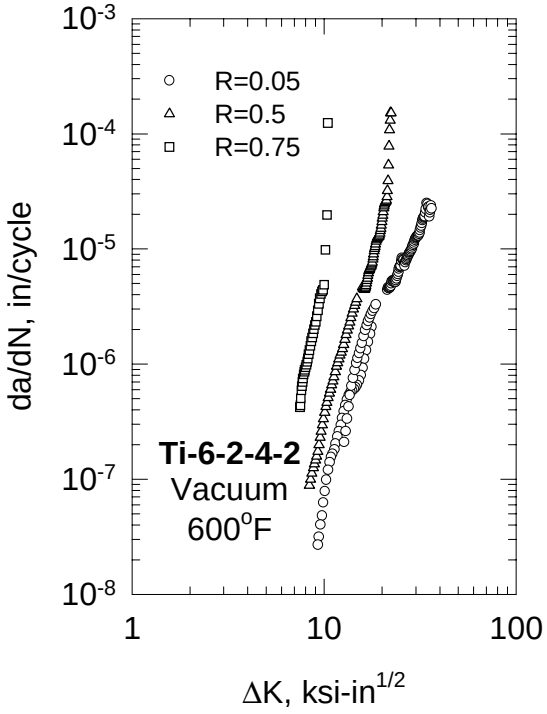

Figure 6. Vacuum FCG data for Ti-6Al-2Sn-4Zr-2Mo+Si at 600°F (316°C)

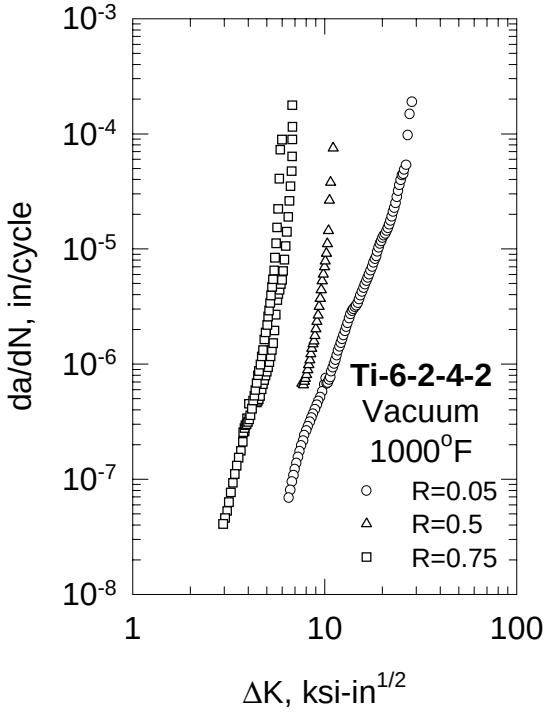

Figure 7. Vacuum FCG data for Ti-6Al-2Sn-4Zr-2Mo+Si at 1000°F (538°C)

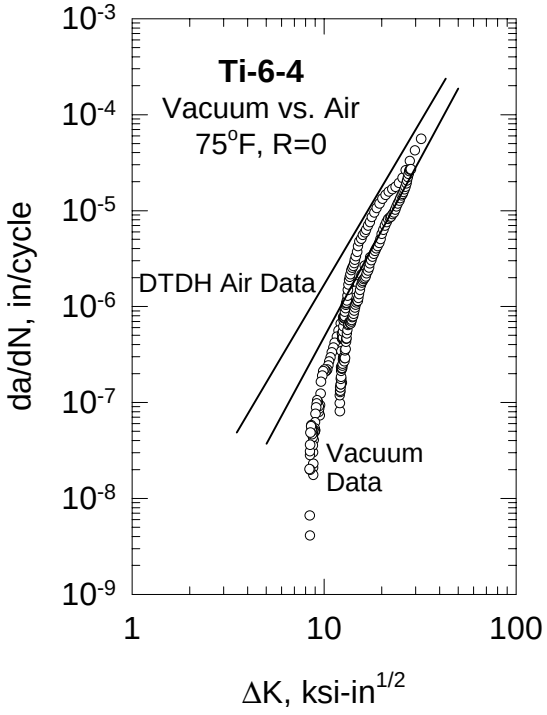

Figure 8. Comparison of vacuum data with air data from DTDH for Ti-6Al-4V at 75°F (24°C) and $R = 0$

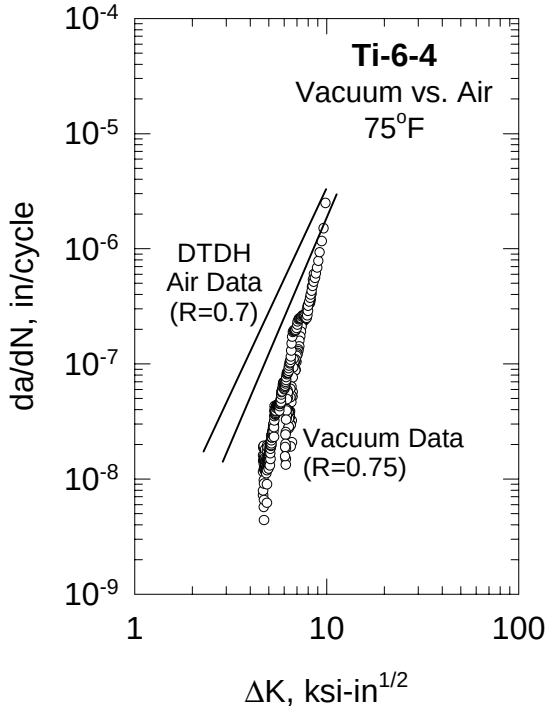

Figure 9. Comparison of vacuum data with air data from DTDH for Ti-6Al-4V at 75°F (24°C) and R = 0.75

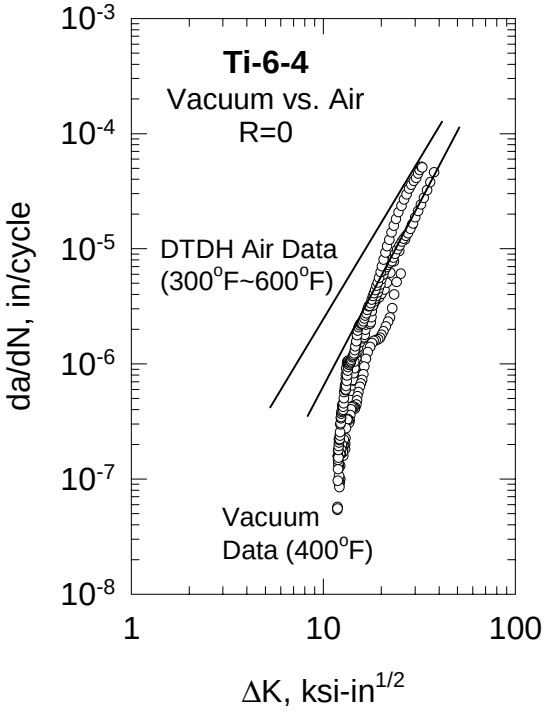

Figure 10. Comparison of vacuum data with air data from DTDH for Ti-6Al-4V at 300-600°F (149-316°C) and R = 0

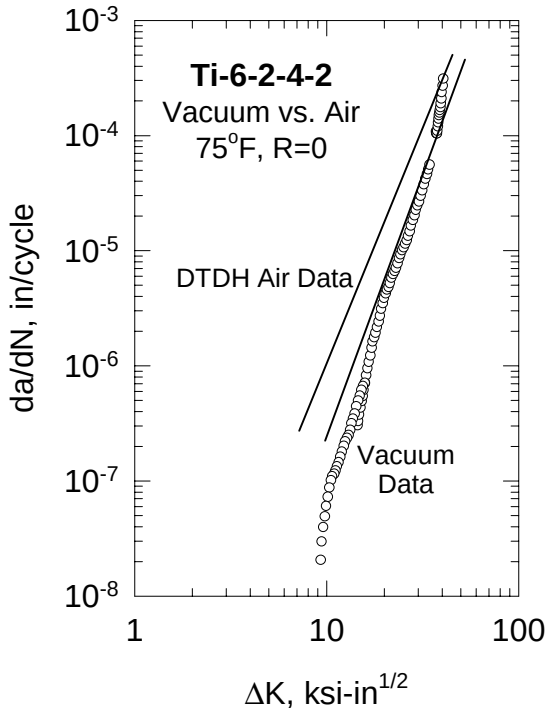

Figure 11. Comparison of vacuum data with air data from DTDH for Ti-6Al-2Sn-4Zr-2Mo+Si at 75°F (24°C) and R = 0

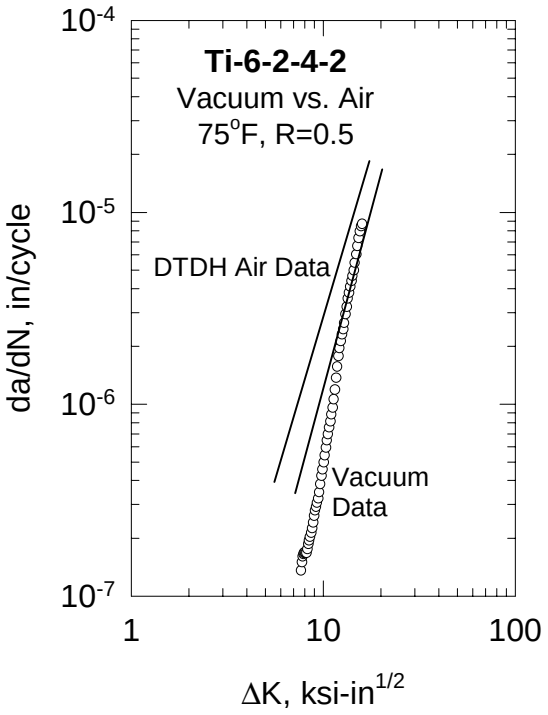

Figure 12. Comparison of vacuum data with air data from DTDH for Ti-6Al-2Sn-4Zr-2Mo+Si at 75°F (24°C) and R = 0.5